

# Accumbal D1R Neurons Projecting to Lateral Hypothalamus Authorize Feeding

## Highlights

- D1R-MSNs comprise the major source of inhibition from accumbens to LH
- Accumbens shell D1R-MSNs reduce activity during feeding
- D1R-MSN activity in LH is causally linked to rapid food intake control
- D1R-MSNs inhibit LH GABA neurons to stop food consumption

## Authors

Eoin C. O'Connor, Yves Kremer, Sandrine Lefort, Masaya Harada, Vincent Pascoli, Clément Rohner, Christian Lüscher

## Correspondence

[christian.luscher@unige.ch](mailto:christian.luscher@unige.ch)

## In Brief

O'Connor et al. find that dopamine D1R-expressing neurons (D1R-MSNs) provide the dominant source of inhibition from accumbens shell to lateral hypothalamus. D1R-MSN activity bidirectionally controls feeding and hypothalamic GABA neurons are identified as a functional target of D1R-MSN inhibition.

# Accumbal D1R Neurons Projecting to Lateral Hypothalamus Authorize Feeding

Eoin C. O'Connor,<sup>1</sup> Yves Kremer,<sup>1</sup> Sandrine Lefort,<sup>1</sup> Masaya Harada,<sup>2</sup> Vincent Pascoli,<sup>1</sup> Clément Rohner,<sup>1</sup> and Christian Lüscher<sup>1,3,\*</sup>

<sup>1</sup>Department of Basic Neurosciences, Medical Faculty, University of Geneva, 1211 Geneva, Switzerland

<sup>2</sup>CREST Project, Medical Innovation Center, Kyoto University Graduate School of Medicine, Kawaharacho 53, Shogoin, Sakyo-ku, Kyoto 606-8509, Japan

<sup>3</sup>Clinic of Neurology, Department of Clinical Neurosciences, Geneva University Hospital, 1211 Geneva, Switzerland

\*Correspondence: [christian.luscher@unige.ch](mailto:christian.luscher@unige.ch)

<http://dx.doi.org/10.1016/j.neuron.2015.09.038>

## SUMMARY

Feeding satisfies metabolic need but is also controlled by external stimuli, like palatability or predator threat. Nucleus accumbens shell (NAcSh) projections to the lateral hypothalamus (LH) are implicated in mediating such feeding control, but the neurons involved and their mechanism of action remain elusive. We show that dopamine D1R-expressing NAcSh neurons (D1R-MSNs) provide the dominant source of accumbal inhibition to LH and provide rapid control over feeding via LH GABA neurons. In freely feeding mice, D1R-MSN activity reduced during consumption, while their optogenetic inhibition prolonged feeding, even in the face of distracting stimuli. Conversely, activation of D1R-MSN terminals in LH was sufficient to abruptly stop ongoing consumption, even during hunger. Direct inhibition of LH GABA neurons, which received input from D1R-MSNs, fully recapitulated these findings. Together, our study resolves a feeding circuit that overrides immediate metabolic need to allow rapid consumption control in response to changing external stimuli.

## INTRODUCTION

The repertoire of feeding behavior is incredibly diverse and incorporates both flexible preparatory actions, like foraging, and highly stereotyped consummatory responses, like mastication. These behavioral sequences must be enacted at appropriate times to fulfill homeostatic energy demands, but consumption also must remain flexible to respond to immediate changes in sensory or environmental conditions. For example, consumption must stop rapidly when foul food is encountered or if predators arise. Such behavior ensures survival, but in excess could lead to anorexia and weight loss. Conversely, when nutritious and palatable foods are found, prolonged consumption can occur in the absence of any immediate metabolic need (Zheng et al., 2009). Such feeding serves to accumulate useful energy stores,

but in many societies the constant availability of energy-dense and palatable foods promotes overeating, leading to weight gain and obesity (Kenny, 2011). Describing neural circuits that can quickly override immediate metabolic need to control consumption in response to changing external conditions represents a necessary step toward identifying causalities in eating disorders and proposing rational treatments.

In the lateral hypothalamus (LH), peripheral and central signals that influence food intake converge to generate an output to midbrain motor pattern generators that subserve the behavioral repertoire of feeding (Anand and Brobeck, 1951; Berthoud, 2004; Delgado and Anand, 1953; Fromentin et al., 2012; Hussain and Bloom, 2013; Kelley et al., 2005b; Morgane, 1969; Schwartz et al., 2000; Wise, 1974). The medial nucleus accumbens shell (NAcSh), which integrates motivational and sensory input, projects to the LH (Thompson and Swanson, 2010; Mogenson et al., 1983), and a series of studies spanning two decades have revealed the importance of this pathway in the control of food consumption (Berthoud, 2004; Kelley et al., 2005a). For example, pharmacological inhibition of the NAcSh in rats and mice triggers intense feeding of both palatable foods and standard chow and leads to neuronal activation in the LH, as detected by expression of the immediate early gene c-Fos (Baldo et al., 2004; Faure et al., 2010; Maldonado-Irizarry et al., 1995; Reynolds and Berridge, 2001; Stratford and Kelley, 1999; Zheng et al., 2003, 2007). Moreover, increased feeding following NAcSh inhibition is prevented by concomitant infusion of a gamma-aminobutyric acid type A (GABA<sub>A</sub>) receptor agonist into the LH (Maldonado-Irizarry et al., 1995; Urstadt et al., 2013). Consistent with these pharmacological studies, unit recordings in freely feeding rats have identified subpopulations of NAcSh neurons that reduce their activity during feeding (Krause et al., 2010; Roitman et al., 2010; Tellez et al., 2012) and that shift to increased firing when animals are presented with aversive conditioned food (Roitman et al., 2010).

From these studies, a model has been proposed in which inhibitory projections from the NAcSh to the LH serve as a sensory sentinel, allowing rapid control over food consumption in response to motivational or sensory signals (Baldo and Kelley, 2007; Kelley et al., 2005b). However, this circuit has not been resolved at the cellular level and its temporal dynamics have not been characterized. For instance, NAcSh inhibitory projection neurons can be classified into two distinct populations

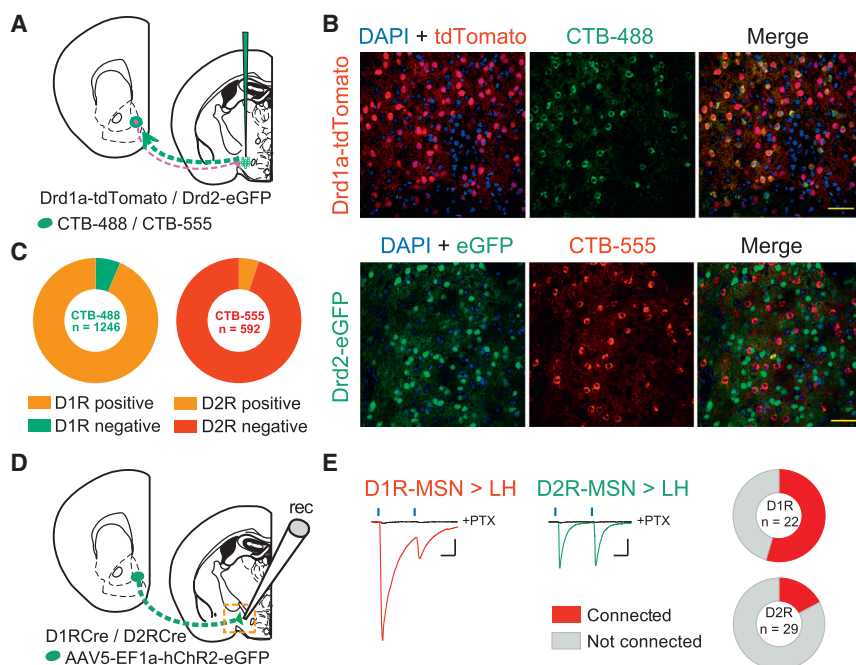


**Figure 1. D1R-MSNs Provide Dominant Accumbal Output to LH**

(A) Schematic for CTB tracing is shown. (B) Representative confocal images from NAcSh, 11 days after CTB injections in LH, are shown. Scale bar, 50  $\mu$ m. (C) Charts show the proportion of CTB-labeled cells in NAcSh colocalizing with D1R-tdTomato (left) or Drd2-eGFP (right). (D) Schematic for optogenetic circuit mapping is shown. (E) Example ex vivo whole-cell recordings from LH neurons, showing 4-ms blue light-evoked inhibitory postsynaptic currents (IPSCs) blocked by picrotoxin (PTX, 50  $\mu$ M, black trace), and connectivity charts are shown. Scale, 200 pA, 20 ms. See also [Figures S1](#) and [S2](#).

according to the dopamine receptor they express ([Bocklisch et al., 2013](#); [Gangarossa et al., 2013](#)), but the dopaminergic receptor identity of NAcSh neurons projecting to the LH is not known ([Heimer et al., 1991](#); [Mogenson et al., 1983](#); [Sano and Yokoi, 2007](#); [Zhang et al., 2013](#)). Second, pharmacological manipulations, electrical stimulation, and unit recordings have lacked the temporal resolution or cell type specificity required to provide a causal link between activity in identified NAcSh-to-LH projection neurons and the control over moment-to-moment food intake. Finally, the LH contains an array of neurons that express different neuropeptides and neurotransmitters ([Schöne and Burdakov, 2012](#)), but the molecular identity of LH neurons receiving inhibitory input from the NAcSh has not been described ([Heimer et al., 1991](#); [Mogenson et al., 1983](#); [Sano and Yokoi, 2007](#); [Zheng et al., 2007](#)).

To address these issues, we established a paradigm in which food consumption could be monitored on a moment-to-moment basis in genetically modified mice, permitting the observation and control of identified cell types. We found that NAcSh D1R-MSNs provide the major source of accumbal inhibition to the LH and reduce their activity during food consumption. Inhibition of D1R-MSNs prolongs feeding in sated mice and even in the face of distracting external stimuli. Conversely, activation of D1R-MSN terminals in LH is sufficient to override immediate metabolic need and rapidly stop food consumption despite hunger. These findings were recapitulated by the direct inhibition of LH GABA neurons, which receive inhibition from D1R-MSNs.

## RESULTS

### D1R-MSNs Provide Dominant NAcSh-to-LH Inhibition

To determine the molecular identity of NAcSh neurons projecting to the LH, we first performed a retrograde tracing study, with in-

jections of cholera-toxin subunit B (CTB) conjugated to a fluorescent dye into the LH of transgenic mice that permit identification of D1R- and D2R-MSNs ([Figures 1A–1C](#)). Injections were focused to the peduncular part of the LH, just lateral to the fornix and ventral to the zona incerta ([Figures S1A](#) and [S1B](#); [Paxinos and Franklin, 2008](#)). Then, 11 days after the injection, coronal slices containing NAcSh were prepared to visualize colocalization of CTB with identified MSNs. Consistent with other neuroanatomical reports ([Thompson and Swanson, 2010](#)), prominent CTB labeling was seen in the medial NAcSh ([Figure S1C](#)). Few labeled cells were found in the NAcSh when CTB injections were made more medially into the anterior hypothalamic area (between the ventricle and the fornix) or more dorsal to the nigrostriatal tract (data not shown).

In *Drd1a*-tdTomato mice ( $n = 3$ ), a total of 1,246 CTB-containing cells (i.e., LH-projecting cells) were counted across the rostro-caudal extent of medial NAcSh. Of these cells, 1,173 (93.6%  $\pm$  0.8%, grouped mean  $\pm$  SEM) were positive for tdTomato, identifying them as D1R-MSNs ([Figures 1B](#) and [1C](#)). Notably, 60.3%  $\pm$  7.7% of D1R-MSNs did not express CTB, likely reflecting cells that project outside of the LH ([Bocklisch et al., 2013](#); [Kupchik et al., 2015](#)) or that the injection of CTB into the LH was unable to seed the entirety of this large structure. At the most rostral and most caudal NAcSh sites, the majority of LH-projecting neurons were identified as D1R-MSNs (minimum 89.7%; [Figure S1D](#)). However, in the bed nucleus stria terminalis (BNST), which lies caudally to the NAcSh and inhibits LH glutamate neurons to increase food intake ([Jennings et al., 2013](#)), only a minority of LH-projecting neurons were positive for tdTomato (for dorsal BNST, grouped mean  $\pm$  SEM, 15.1%  $\pm$  3.1%; for ventral BNST, 22.8%  $\pm$  3.5%,  $n = 5$ ; [Figure S2](#)). Consistent with findings in *Drd1a*-tdTomato mice, in *Drd2*-eGFP animals ( $n = 2$ ), a total of 593 CTB-positive cells were counted in the NAcSh, with only 29 cells (5.2%  $\pm$  1.1%, grouped mean  $\pm$  SEM) positive for eGFP ([Figures 1B](#) and [1C](#)). Taken together, these tracing studies show that the dominant projection from NAcSh to LH comprises D1R-MSNs.

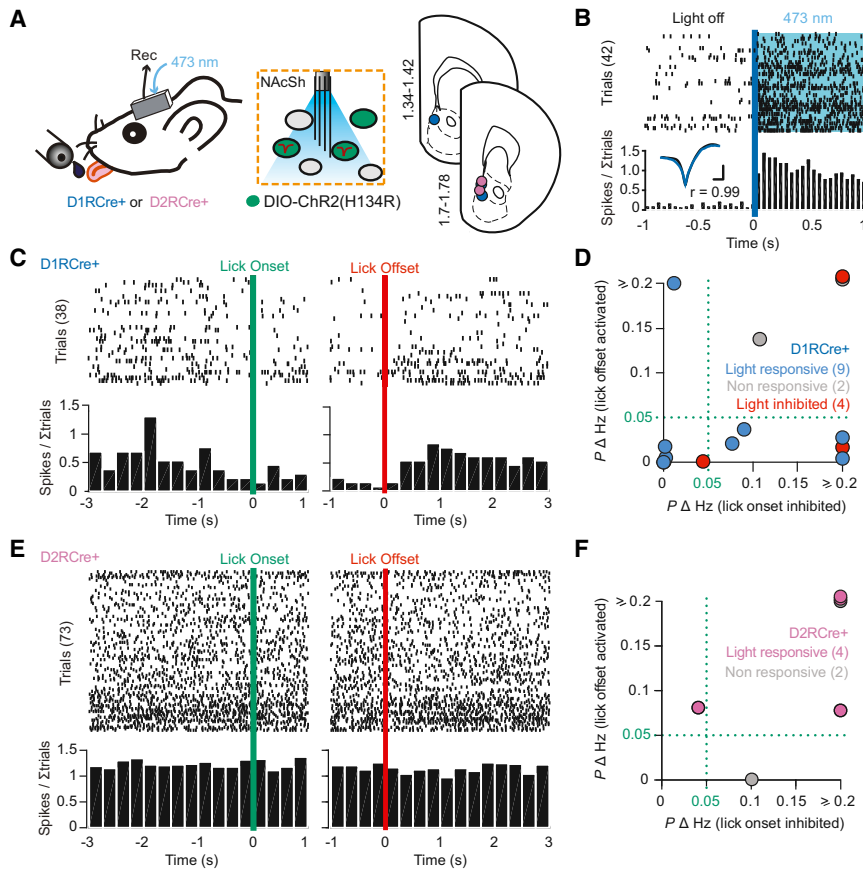


## Figure 2. D1R-MSNs Reduce Firing during Food Consumption

(A) Schematic of in vivo unit recordings and recording sites (right; millimeters from bregma) (Paxinos and Franklin, 2008) is shown.

(B) Example light-responsive unit in D1R-Cre+ mouse (i.e., D1R-MSN). Peri-stimulus time histogram (PSTH) shows single-unit activity and mean spike waveform (inset; scale, 200  $\mu$ s, 100  $\mu$ V) prior to and during 1-s continuous blue light stimulation. Bin size, 50 ms.

(C) For the same unit shown in (B), PSTH of activity aligned to consumption onset (left) and offset (right). Activity tended to reduce during onset ( $p = 0.07$ , Wilcoxon rank-sum test) and significantly increased during lick offset ( $p < 0.05$ ). Bin size, 250 ms.

(D) Plot of all recorded units in D1R-Cre+ mice according to significance level (Wilcoxon rank-sum test) of activity change during lick offset versus onset is shown.

(E) As for (C), except for a light-responsive unit obtained from a D2R-Cre mouse. Activity of this unit did not change across lick onset or offset.

(F) As for (D), but units obtained from D2R-Cre mice are shown.

See also Figure S3.

## D1R-MSN Inhibitions Permit Food Consumption

Following our neuroanatomical data and based on prior descriptions of NAcSh-to-LH circuitry (Berthoud, 2004; Kelley et al., 2005a; Krause et al., 2010; Roitman et al., 2010; Tellez et al., 2012), we predicted that D1R-MSN activity would reduce during food consumption, thus relieving inhibition from downstream LH neurons to authorize feeding. To test this prediction, we undertook in vivo unit recordings of optogenetically identified NAcSh D1R-MSNs in mice that were freely feeding a palatable liquid fat solution from a sipper tube (5% v/v Lipofundin in water; Figures 2A–2D and S2). Licks on the sipper tube were recorded with a lickometer, allowing the onset and offset of individual feeding events, termed bursts, to be monitored with high temporal resolution.

Consistent with a permissive role in food intake control, the majority of optogenetically identified NAcSh D1R-MSNs reduced their activity during consumption onset ( $n = 5/9$ ,  $p < 0.05$  and  $n = 2/9$ ,  $p < 0.1$ ; Wilcoxon rank-sum test) and increased their activity concomitantly with consumption offset ( $n = 8/9$ ,  $p < 0.05$ ) (Figures 2B–2D and S3B). Non-light-responsive units ( $n = 2$ ) showed no change in activity in relation to consumption onset or offset (Figures 2D, S3B, and S3C). We also recorded units that were inhibited by blue light ( $n = 4$ ; Figures 2D, S3B, and S3D). Half of the light-inhibited units reduced activity during feeding onset and increased activity with feeding offset ( $p < 0.05$ ), while the remaining units showed no change in activity during consumption onset. While we cannot be certain as to the identity of light-inhibited units, this response most likely arose from local recurrent collateral inhibition, which, in the dorsal

To explore the functional nature of the NAcSh-to-LH connection, an optogenetic-assisted circuit mapping approach was employed. First, the blue light-activated cation channel, channelrhodopsin (ChR2(H134R)), was expressed in D1R- or D2R-MSNs by injecting an adeno-associated virus (AAV) harboring a floxed-ChR2(H134R) construct into the NAcSh of D1R-Cre or D2R-Cre mice, respectively (Figures 1D and 1E). After 2 weeks, allowing time for ChR2(H134R) expression, acute coronal brain slices containing LH were prepared for ex vivo electrophysiology recordings. Cells in the LH were randomly patched while monitoring blue light-evoked inhibitory postsynaptic currents (IPSCs) derived from D1R-MSN or D2R-MSN afferents. We observed that few ChR2(H134R)-eYFP-expressing fibers were present in the LH of D2R-Cre mice compared to D1R-Cre mice (Figure 4B). In D1R-Cre mice, light-evoked postsynaptic currents could be recorded in 56% of LH neurons (15 of 27 neurons,  $n = 3$  mice; mean amplitude  $\pm$  SEM, 630  $\pm$  334 pA) that were blocked with picrotoxin (Figure 1E). This finding is consistent with previous in vivo recordings in rats, where 52.5% of subpallidal neurons received accumbal inhibition (Mogenson et al., 1983). By comparison, only 17% of LH neurons received inhibition from NAcSh D2R-MSNs (5 of 29 neurons,  $n = 3$  mice; mean amplitude  $\pm$  SEM, 177  $\pm$  79 pA). Taken together, these data support neuronal tracing studies to show that D1R-MSNs comprise the dominant source of accumbal inhibition to the LH.

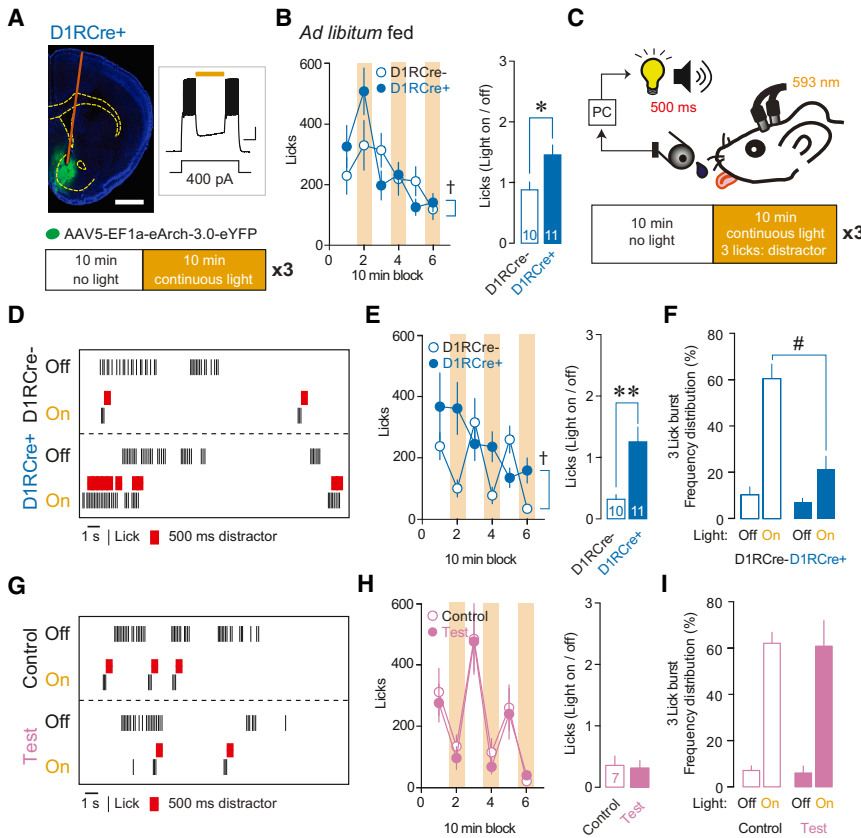


**Figure 3. D1R-MSNs Inhibitions Prolong Food Intake**

(A) Schematic of experiment, with representative image of eArch-3.0-eYFP infection in a D1RCre+ mouse (orange line shows fiber tract; scale, 1 mm). Ex vivo, whole-cell recording from NAcSh eYFP+ neuron is superimposed, with inhibition of current evoked spiking by orange light shown (scale, 20 mV, 200 ms; RMP, -92 mV).

(B) Food intake is shown across time (left; orange segments show light on), together with total intake (right), as a function of activity in light-on blocks divided by the light-off blocks. †ANOVA, condition (D1RCre-, D1RCre+) × light (off, on) interaction,  $F(1,19) = 5.55$ ,  $p < 0.05$ .

(C) Schematic of stimulus distraction test is shown. (D) Example lick histograms from distraction test are shown.

(E) As is shown for (B), except for the distraction test. †ANOVA, condition × light interaction,  $F(1,19) = 8.36$ ,  $p < 0.01$ .

(F) Frequency distribution of three-lick bursts. # $p < 0.025$ , non-paired, two-tailed t test (Bonferroni correction), following ANOVA, condition × light interaction,  $F(1,19) = 16.55$ ,  $p \leq 0.001$ .

(G–I) As for (D)–(F), except that eArch-3.0-eYFP was expressed in D2R NAcSh neurons (D2RCre+ mice).

\* $p < 0.05$ , \*\* $p < 0.01$ , non-paired, two-tailed t test. Error bars, SEM. See also Figures S4 and S6.

striatum, is most common within D1R- or D2R-MSNs than between D1R- and D2R-MSNs (Taverna et al., 2008). To contrast the activity of D1R-MSNs, we repeated in vivo unit-recording experiments in optogenetically identified D2R-expressing NAcSh neurons (D2RCre+ mice; Figures 2E, 2F, S3E, and S3F). D2R-expressing neurons did not reliably change activity in line with consumption onset (smallest  $p = 0.33$  for  $n = 3/4$ , Wilcoxon rank-sum test) or offset (smallest  $p = 0.08$  for  $n = 4/4$ ). Taken together, unit-recording data suggest that NAcSh D1R-MSN activity reductions were key for allowing food intake, while D1R-MSN activity increases serve to stop and shift behavior away from feeding.

Since the observed reductions in D1R-MSN activity that parallel food consumption are only correlational, we sought causal evidence by asking first if discrete photoinhibition of NAcSh D1R-MSNs could promote feeding. The orange light-gated inhibitory proton pump, eArch-3.0, was virally expressed in D1R-MSNs and fiber optics implanted targeting the NAcSh (Figures 3A and S6A). Whole-cell recordings of infected NAcSh neurons ex vivo confirmed that orange light illumination inhibited action potentials normally evoked by positive current injection (Figure 3A). In ad-libitum-fed D1RCre+ mice, orange light illumination of the NAcSh significantly increased liquid fat intake, compared to Cre- littermates that did not express eArch-3.0 (Figure 3B). Thus, a reduction in NAcSh D1R-MSN activity was sufficient to promote palatable food consumption, even when there was no immediate metabolic need to feed.

We further questioned whether D1R-MSNs could fulfill the role of sensory sentinel previously ascribed to the NAcSh (Kelley et al., 2005a), by rapidly adjusting food intake in response to changing external conditions. To this end, we combined eArch-3.0-mediated optogenetic inhibition experiments with an unexpected stimulus distraction test (Figures 3C–3F). During alternating 10-min blocks of a 1-hr fat consumption session, feeding burst initiation was monitored in real time and triggered the presentation of a brief distractor stimulus (i.e., three consecutive licks, with interlick intervals (LLIs) of  $\leq 1$  s, triggered a 500-ms auditory/visual stimulus; Figure 3C). In control mice, the distractor stimulus was efficient in rapidly stopping ongoing consumption from one lick to the next, as shown by an increase in the frequency of bursts comprising only three licks (Figures 3D–3F). However, photoinhibition of D1R-MSNs led to a significant reduction in the efficiency of the distractor stimulus to stop ongoing feeding (Figures 3D–3F). To explore whether this result was unique to D1R-MSN inhibition, stimulus distraction experiments were repeated, but now with eArch-3.0-mediated inhibition of D2R-expressing NAcSh neurons (Figures 3G–3I and S4). As expected from the non-reactivity of these cells in unit-recording observations, photoinhibition of D2R-expressing NAcSh neurons did not alter the efficiency of a distractor stimulus to stop ongoing feeding (Figures 3G–3I).

Collectively, these data show that reductions in NAcSh D1R-MSN activity are permissive for feeding and suggest that increases in D1R-MSN activity are required to rapidly stop and

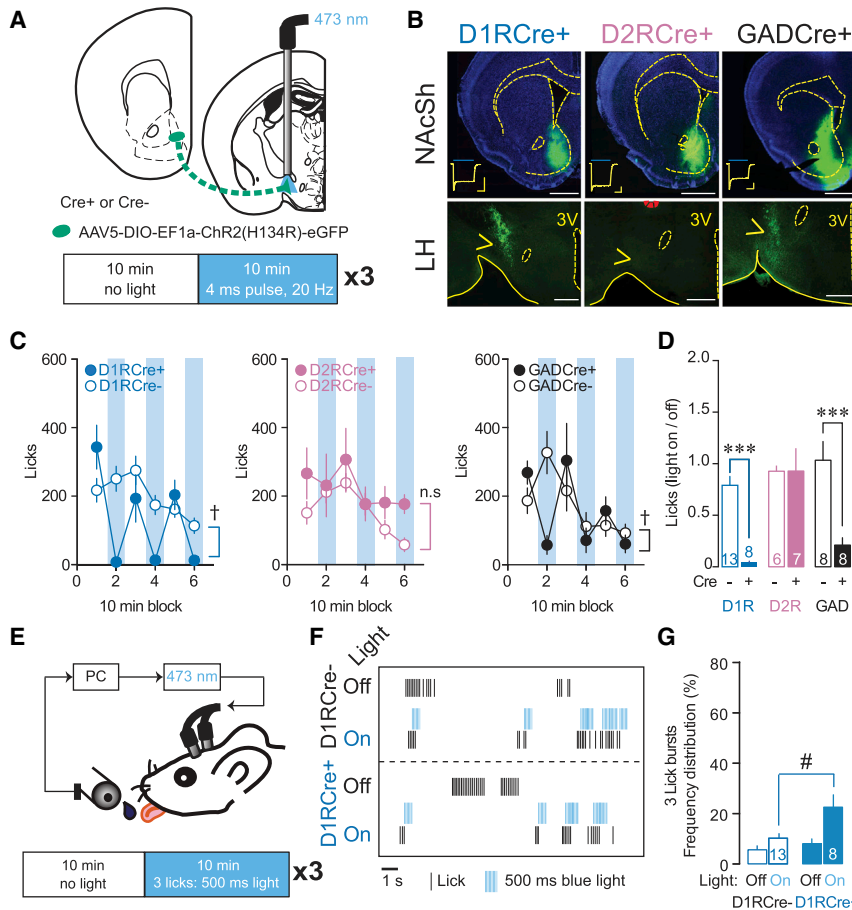


**Figure 4. Activation of D1R-MSN Terminals in LH Rapidly Stops Feeding**

(A) Schematic of experiment is shown. (B) Example images of NAcSh ChR2(H134R)-eYFP infections (top; scale, 1 mm). Photocurrents in response to 300-ms blue light stimulation; recorded ex vivo from infected NAcSh neurons are superimposed (scale, 100 pA, 100 ms). Prominent fiber terminals are seen in the LH of D1RCre and GADCre, but not D2RCre mice (bottom; arrowhead indicates LH; scale bar, 500  $\mu$ m). (C) Food intake across time (blue segments show light on) is shown.  $\dagger p < 0.01$ , ANOVA, condition (Cre+, Cre-)  $\times$  light (off, on) interaction. Note mice were fed ad libitum. (D) Total intake is shown, as a function of activity in light-on blocks divided by the light-off blocks.  $***p \leq 0.001$ , non-paired, two-tailed t test. (E) Schematic for closed-loop optogenetic experiment (mice fed ad libitum) is shown. (F) Example lick histograms from closed-loop optogenetic test are shown. (G) Frequency of three-lick bursts during light-off and -on periods.  $\#p < 0.025$ , non-paired, two-tailed t test (Bonferroni correction), following ANOVA, condition  $\times$  light interaction,  $F(1,19) = 6.26$ ,  $p < 0.05$ . Error bars, SEM. See also [Figures S5](#) and [S6](#).

shift behavior away from consumption in response to salient external stimuli.

### D1R-MSN Projections to the LH Authorize Feeding

Thus far, D1R-MSNs were observed and manipulated at the somatic level in NAcSh. If D1R-MSN activity was causally related to feeding owing to downstream inhibition in the LH, then this could be demonstrated in two ways. First, forcing activation of NAcSh D1R-MSN terminals in the LH should be sufficient to prevent consumption from occurring, even during hunger. Second, in line with findings from the stimulus distraction test, activation of D1R-MSN terminals in the LH should be sufficient to rapidly stop ongoing feeding from one moment to the next.

To test the first prediction, ChR2(H134R) was expressed selectively in NAcSh D1R-MSNs with implanted fiber optics now targeting D1R-MSN terminals in the LH (D1RCre mice; [Figures 4A](#), [4B](#), and [S6C](#)). Blue light stimulation (20 Hz, 4-ms pulses) of D1R-MSN terminals in the LH strongly suppressed fat intake in ad-libitum-fed D1RCre+ mice, compared to Cre- littermate controls that did not express ChR2(H134R) ([Figures 4C](#) and [4D](#)). This effect was not specific to fat, as optogenetic stimulation of D1R-MSN terminals in the LH also suppressed liquid sucrose consumption in a separate cohort of mice ([Figures S5A](#), [S5B](#), and [S6F](#)). Importantly, blue light stimulation

also was efficient to suppress fat intake in mice that were food deprived for 24 hr prior to the test ([Figure S5C](#)). Thus, activation of D1R-MSN terminals in the LH is sufficient to suppress food intake, even despite a state of hunger.

Since neuronal tracing identified a small proportion of NAcSh neurons projecting to the LH as D2R-MSNs ([Figure 1](#)), we examined whether stimulating D2R-MSN terminals in the LH would, nevertheless, be sufficient to alter feeding. Behavioral optogenetic experiments were repeated but now with stimulation of ChR2(H134R)-infected NAcSh D2R-MSN terminals in the LH (D2RCre mice; [Figures 4A–4D](#) and [S6D](#)). Optogenetic stimulation of D2R-MSN terminals in the LH during 10-min periods had no effect on food consumption in ad-libitum-fed mice ([Figures 4A–4D](#)).

As an additional control, optogenetic experiments were repeated in a mouse line that allowed stimulation of all GABAergic NAcSh projections to the LH (GADCre mice; [Figures 4A–4D](#) and [S6E](#)). Mimicking results with stimulation of D1R-MSN terminals in the LH, blue light stimulation of all inhibitory NAcSh projections to the LH suppressed feeding in ad-libitum-fed GADCre+ mice compared to Cre- controls ([Figures 4C](#) and [4D](#)). Collectively, these experiments add functional relevance to neuronal tracing and in vivo unit-recording data by demonstrating causality between the activity of D1R-MSNs projecting to the LH and rapid consumption control in a manner that can override immediate metabolic need.

Would activation of the D1R-MSN-to-LH pathway also be sufficient to rapidly stop the highly stereotyped action of licking once food consumption had been initiated, akin to the effect

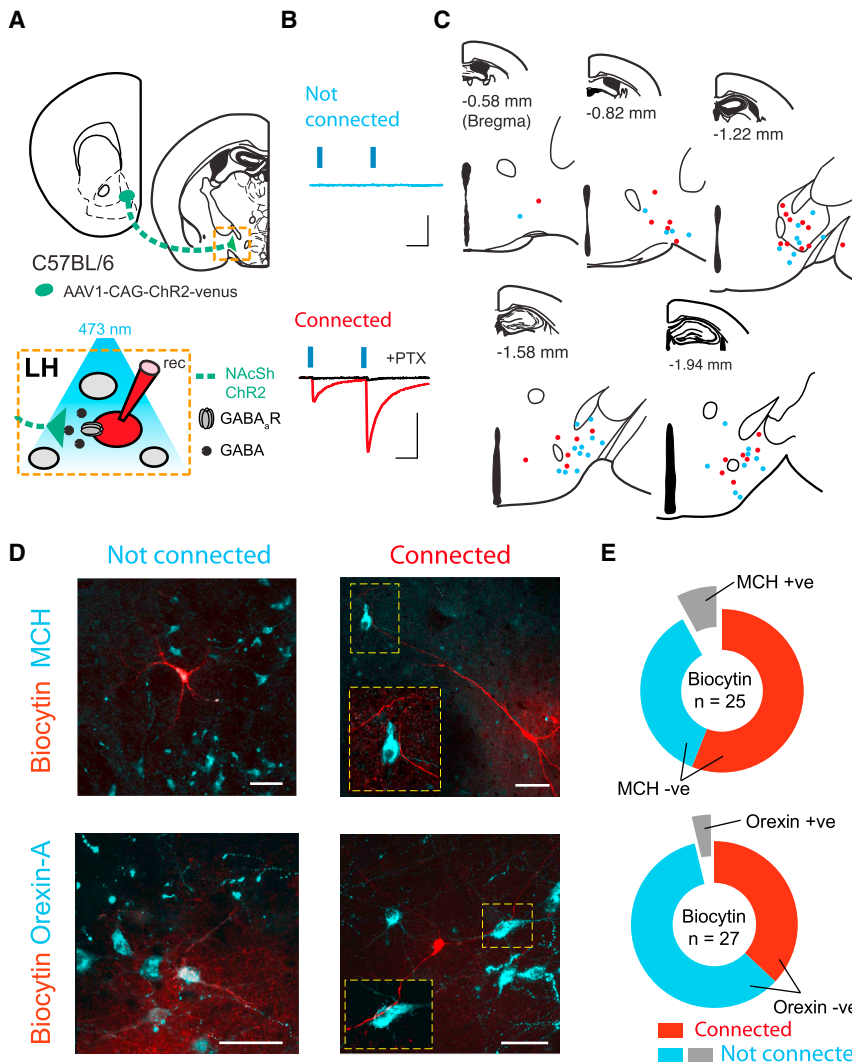


**Figure 5. Accumbens Inhibits Non-orexin-A and Non-MCH Neurons in LH**

(A) Schematic of experiment. Note non-floxed ChR2 was expressed in wild-type mice.

(B) Example traces (average of 20 sweeps) from a not-connected LH neuron, not responding to blue light ( $2 \times 4$ -ms duration, 50-ms interval; top), and a second connected neuron where blue light evoked postsynaptic currents (bottom) that were sensitive to picrotoxin (PTX;  $50 \mu\text{M}$ ; black trace) are shown. Scale, 20 ms, 200 pA. Stimulation artifacts were removed.

(C) The location of connected (red dots) and not-connected (blue dots) biocytin-filled neurons across the rostro-caudal extent of the LH. Sections were redrawn from Paxinos and Franklin (2008).

(D) Example images of not-connected biocytin-filled neurons (left) that were also positive for MCH (top) or orexin-A (bottom) and connected neurons (right) that were negative for MCH or orexin-A. Inserts show processes that made appositions with nearby MCH- or orexin-A-positive neurons. Scale bars,  $50 \mu\text{M}$ .

(E) Summary connectivity charts for filled neurons stained against MCH (top) or orexin-A (bottom) are shown.

### NAcSh Targets Non-MCH and Non-orexin LH Neurons

Which LH neurons receive inhibition from the NAcSh? To address this question, we again adopted an unbiased optogenetic-assisted circuit-mapping approach, monitoring light-evoked IPSCs in LH neurons derived from NAcSh afferents expressing non-floxed ChR2 (Figure 5). On this occasion, biocytin was added to the recording pipette to allow subsequent localization and immunohistochemical

seen with an external distractor stimulus? To test this possibility, we developed a closed-loop optogenetic intervention in which feeding burst initiation was monitored in real time and now triggered brief blue light stimulation of D1R-MSN terminals in the LH (i.e., three consecutive licks, with ILIs  $\leq 1$  s, triggered a 500-ms train of blue light; 20 Hz, 4-ms pulse; Figure 4E). This intervention was restricted to 10-min light-on periods, which alternated with 10-min light-off periods. The frequency of three-lick bursts significantly increased during the light-on period in D1RCre+ mice versus controls, confirming that brief activation of D1R-MSN terminals in the LH was sufficient to rapidly inhibit consumption from one lick to the next (Figures 4E–4G). Delivering only a single 4-ms pulse following burst initiation had no effect on the frequency of three-lick bursts (Figures S5D–S5F), suggesting that relatively sustained inhibition of LH neurons is required to stop ongoing feeding. The ability of this discrete manipulation to interrupt the highly stereotyped motor action of licking exemplifies the tight control that NAcSh D1R-MSNs projecting to the LH exert over consummatory behavior.

identification of recorded neurons. Initially, we screened for neurons containing the peptides orexin/hypocretin or melanin-concentrating hormone (MCH), since their activity is largely associated with promoting feeding (de Lecea et al., 1998; Qu et al., 1996; Sakurai et al., 1998).

Using this method, a total of 62 LH neurons in wild-type mice were labeled with biocytin, of which 29 (47%) received light-evoked IPSCs from NAcSh afferents (connected cells; Figure 5B). Connected neurons were distributed throughout the rostro-caudal extent of the LH and were intermingled with non-connected neurons (Figure 5C). Biocytin-labeled neurons ( $n = 25$ ) were stained against MCH (Figures 5D and 5E). Of these neurons, 14 were connected, but none of these were positive for MCH. Only two neurons were positive for MCH, but these were not connected. Another 27 biocytin-labeled neurons were stained against orexin-A to identify orexin/hypocretin cells (Figures 5D and 5E). Of these neurons, ten were connected, but none of these were positive for orexin-A. Only one neuron was identified as positive for orexin-A, but it was not connected. Notably, some connected neurons were observed to make

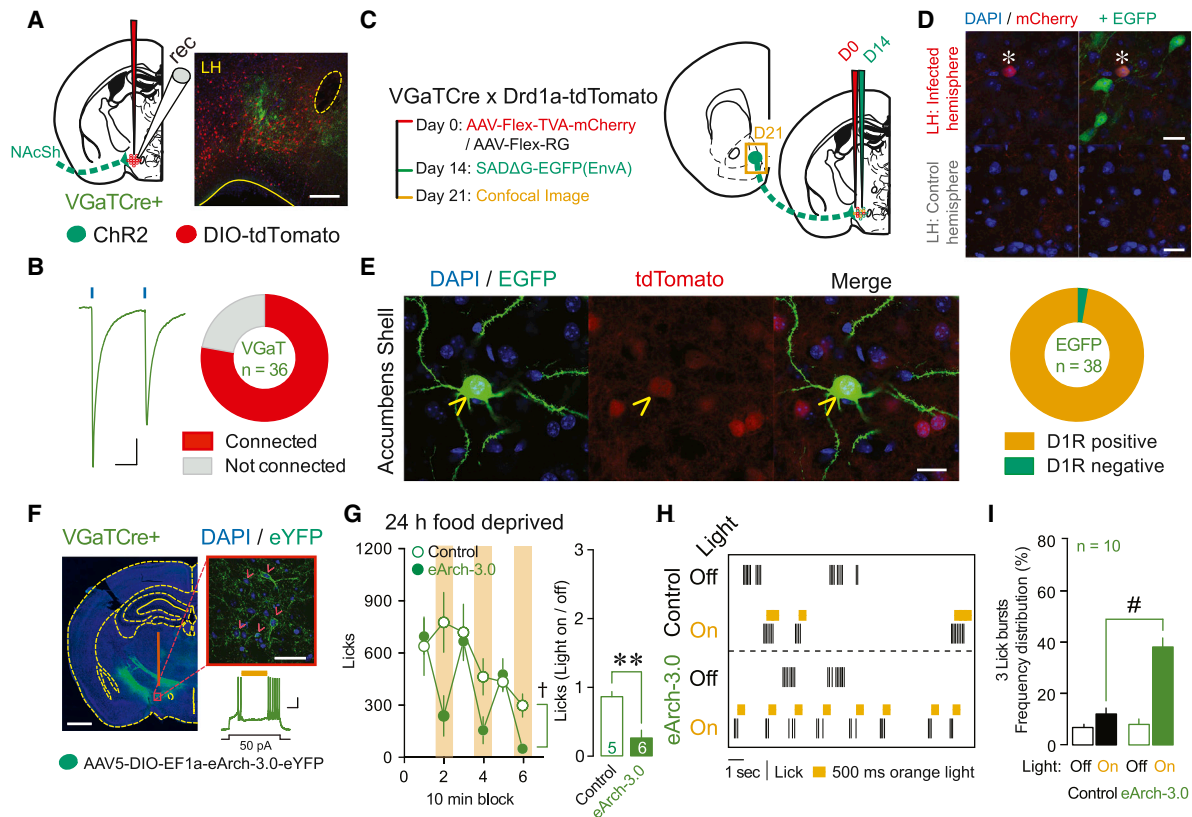


**Figure 6. D1R-MSNs Inhibit LH GABA Neurons to Rapidly Stop Feeding**

(A) Schematic for cell-type-specific circuit mapping, with example image of LH preparation (right; scale bar, 200  $\mu$ M). Note non-floxed ChR2 was expressed in the NAcSh of VGATCre+ mice.

(B) Example whole-cell recording from connected, identified LH VGAT neuron in response to blue light stimulation of NAcSh afferents ( $2 \times 4$ -ms pulse, 50-ms interval; scale, 20 ms, 200 pA) and connectivity chart are shown.

(C) Schematic for modified rabies tracing is shown.

(D) Representative confocal image shows a starter neuron in LH (\*, top), with image from the control hemisphere (bottom), taken in the same slice and with the same imaging settings. Scale bars, 20  $\mu$ m.

(E) Representative image of an EGFP-labeled neuron in NAcSh, which is also positive for tdTomato (i.e., D1R-MSN; scale bar, 20  $\mu$ m) and summary colocalization chart (quantification from  $n = 2$  mice) are shown.

(F) Example image of LH eArch-3.0-eYFP infection in a VGATCre+ mouse (red line shows fiber tract; scale, 1 mm). Zoom shows eYFP+ LH neurons (right; indicated by arrowheads; scale bar, 50  $\mu$ m). Ex vivo, whole-cell recording from LH eYFP+ neuron showing orange light inhibition of positive current-evoked spiking (bottom; scale 20 mV, 200 ms).

(G) Food intake is shown across time (left; orange segments indicate light on), with total intake as a function of activity in light-on blocks divided by light-off blocks (right).  $\dagger$ ANOVA, condition (control, eArch-3.0)  $\times$  light (off, on) interaction,  $F(1,9) = 8.64$ ,  $p < 0.05$ .  $**p < 0.01$ , non-paired, two-tailed t test.

(H) Example lick histograms from a single VGATCre+ mouse undertaking closed-loop optogenetic experiments are shown.

(I) Frequency distribution of three-lick bursts during the light-off and -on periods, in control and test (eArch-3.0) sessions, is shown.  $\#p < 0.025$ , paired, two-tailed t test (Bonferroni correction), following ANOVA, condition  $\times$  light interaction,  $F(1,9) = 86.6$ ,  $p < 0.001$ .

Error bars, SEM. See also Figure S6.

appositions with nearby MCH- or orexin-A-positive neurons (Figure 5D), suggesting that connected LH neurons may serve as an additional gate between MCH and orexin/hypocretin neurons and accumbal input (Sano and Yokoi, 2007). Thus, our findings point to other LH cell types as the major target of NAcSh inhibition.

### D1R-MSNs Inhibit LH GABA Neurons

LH neurons that increased their calcium activity during feeding of high-fat chow, grain-based chow, or calorie-dense liquid were marked by expression of the vesicular GABA transporter

(VGAT) (Jennings et al., 2015). Similarly, stimulation of LH GABA neuron terminals in the ventral tegmental area (VTA) increased intake of moist chow and generated maladaptive consummatory behavior (Nieh et al., 2015). We therefore postulated that direct inhibition of LH GABA neurons could provide one mechanism through which D1R-MSNs rapidly control food consumption.

To examine whether LH GABA neurons received accumbal inhibition, LH neurons of VGATCre+ mice were tagged with a virally expressed, floxed fluorescent reporter protein and NAcSh afferents were infected with non-floxed ChR2 (Figure 6A). This

preparation allowed selective targeting of LH GABA neurons for ex vivo whole-cell recordings, while simultaneously monitoring light-evoked IPSCs derived from NAcSh afferents. Of all LH GABA neurons recorded, 78% were connected (28 of 36 cells;  $n = 3$  mice; mean amplitude  $\pm$  SEM of  $803 \pm 217$  pA; [Figure 6B](#)), suggesting enriched targeting of this LH neuronal population by accumbens.

While this preparation revealed functional inhibition from NAcSh to LH GABA neurons, it could not be used to selectively restrict ChR2 expression to D1R- or D2R-MSNs, as Cre was expressed in all VGaT neurons. To circumvent this problem, we generated a new mouse line that allowed selective targeting of LH GABA neurons together with identification of D1R-MSNs in the same animals (VGaT-Cre  $\times$  *Drd1a*-tdTomato mice). In these mice, we performed modified rabies tracing to identify monosynaptic inputs from NAcSh onto LH GABA neurons ([Figure 6C](#)). First, the Cre-inducible avian sarcoma leucosis virus glycoprotein EnvA receptor (TVA) and rabies virus envelope glycoprotein (RG) were targeted unilaterally to LH GABA neurons ([Figures 6C and 6D](#)), allowing rabies virus infection and monosynaptic retrograde transport, respectively, from these starter neurons ([Jennings et al., 2013; Watabe-Uchida et al., 2012; Wickersham et al., 2007](#)). Then, 2 weeks later, the modified rabies virus SADΔG-EGFP(EnvA) was injected unilaterally into the LH and 1 week later slices of NAcSh were prepared for confocal imaging. EGFP-labeled neurons with spiny morphologies were present in NAcSh ([Figure 6E](#)), confirming a monosynaptic projection from MSNs to LH GABA neurons. Moreover, 97% of these EGFP neurons also were positive for tdTomato, identifying them as D1R-MSNs ([Figure 6E](#)). Taken together, these studies demonstrate monosynaptic inhibition from NAcSh D1R-MSNs to LH GABA neurons.

If activating inhibitory NAcSh D1R-MSN projections in the LH is sufficient to stop food consumption, then this finding should be recapitulated by direct inhibition of the relevant postsynaptic target cell type in the LH. Indeed, after 24 hr of food deprivation, direct inhibition of LH GABA neurons, achieved by photoactivation of eArch-3.0 selectively in LH VGaT+ cells, was sufficient to suppress liquid fat consumption ([Figures 6F, 6G, and S6G](#)). Moreover, using our closed-loop optogenetic intervention, brief photoinhibition (500 ms) of LH GABA neurons also was sufficient to rapidly stop ongoing consumption from one lick to the next ([Figures 6H and 6I](#)). These findings thus fully replicated effects on feeding behavior observed following stimulation of D1R-MSN terminals in the LH. Therefore, while these experiments do not formally exclude the contribution of D1R-MSN collaterals to other structures in feeding control (such as the ventral pallidum [VP]), they demonstrate sufficiency of LH GABA neuron inhibitions to effectuate NAcSh D1R-MSN output.

Collectively, these data add to a growing body of literature recognizing the importance of LH GABA neurons in controlling consummatory actions ([Jennings et al., 2015; Nieh et al., 2015](#)), most likely irrespective of a food's nutritional content or palatability, and they suggest that inhibition from upstream D1R-MSNs provides critical temporal control over when consummatory actions should start and stop in response to changing external stimuli.

## DISCUSSION

Building on a long-standing observation that the NAcSh-to-LH pathway regulates feeding ([Baldo et al., 2004; Berthoud, 2004; Faure et al., 2010; Kelley et al., 2005a; Maldonado-Irizarry et al., 1995; Reynolds and Berridge, 2001; Stratford and Kelley, 1999; Urstadt et al., 2013; Zheng et al., 2003](#)), our study identified D1R-MSNs as the major route through which consumption control is conveyed between these neural nodes. Using in vivo recordings, we found that NAcSh D1R-MSN activity reduces during food intake and increases concomitant with feeding cessation. With optogenetics, we demonstrated causality between the activity of D1R-MSNs and rapid consumption control. Finally, we identified inhibition of LH GABA neurons by D1R-MSNs as an important mechanism allowing for temporally precise regulation of consummatory actions. Taken together, our data both advance and provide critical support for the notion that NAcSh serves as a sensory sentinel over food consumption ([Kelley et al., 2005b](#)).

The focus of this report was on output from NAcSh to LH; however, accumbal D1R-MSNs also project to other brain areas including the VP ([Kupchik et al., 2015](#)) and the VTA ([Bocklisch et al., 2013](#)). Accumbal output to the VP has been well described in relation to feeding ([Stratford and Wirtshafter, 2012](#)), although little is known about the discrete functions of D1R- or D2R-MSNs in this pathway. One possibility is that D1R-MSN projections to the VP perform a similar function to those that project to the LH. Indeed, single-axon tracing suggests that accumbal neurons with terminal fields in LH also may give off collaterals to the VP ([Tripathi et al., 2010](#)). Alternatively, neurons from the NAcSh to the VP may specialize in hedonic processing related to feeding, a function that seems particular for the VP rather than the LH ([Cromwell and Berridge, 1993](#)). Understanding the complete molecular identity of NAcSh postsynaptic partners in the VP and to what extent functional collaterals exist between the VP- and LH-projecting MSNs will go some way to resolving this circuit. Regarding the VTA, could D1R-MSN projections to this structure be responsible for the effects on feeding that we report here? We think this is unlikely for two reasons. First, neuroanatomical reports indicate that, compared to the LH, the VTA represents a relatively minor output from medial NAcSh ([Thompson and Swanson, 2010](#)). Second, direct activation of VTA GABA neurons, of which over 87% receive accumbal inhibition ([Bocklisch et al., 2013](#)), actually stops food consumption ([van Zessen et al., 2012](#)). These results stand in opposition to our findings, whereby reducing D1R-MSN activity serves to promote feeding. Thus, we favor D1R-MSN projections to the LH, rather than the VTA, as a key output pathway relevant for consumption control.

Functional gradients across the rostro-caudal extent of the NAcSh have been described. For example, microinfusions of AMPAR antagonists that generate appetitive feeding in the rostral NAcSh require D1R signaling, while the same treatment in caudal NAcSh generates fear and requires both D1R and D2R signaling ([Richard and Berridge, 2011](#)). Such gradients could reflect divergent input-output relationships between rostral and caudal NAcSh. However, in our tracing study, the dominant NAcSh projection to the LH comprised D1R-MSNs

at both the most rostral and most caudal sites. Surprisingly, in the BNST, which lies in continuity with caudal NAcSh, the dopamine receptor expression of LH projection neurons flipped, with only a minority of these neurons expressing D1Rs. This finding could offer one account for functional differences between studies of rostral and caudal NAcSh, which also may incorporate anterior aspects of BNST. Moreover, the differential expression of D1Rs on LH projections from NAcSh versus BNST provides further understanding as to how these two inhibitory pathways play opposite roles in food intake control (Jennings et al., 2013).

In addition to food consumption, the NAcSh has been appreciated for its role in other motivated behaviors, including conditioned reinforcement, Pavlovian-to-instrumental transfer and instrumental response selection (Cardinal et al., 2002), hedonic reactivity (Faure et al., 2010), taste aversion (Roitman et al., 2010), fear (Reynolds and Berridge, 2001), psychomotor sensitization (Smith et al., 2013), pair bonding (Aragona et al., 2006), and social play (van Kerkhof et al., 2014). Given the substantial nature of the NAcSh-to-LH projection, its function likely extends beyond only consumption control. Indeed, calcium imaging of LH GABA neurons has identified functionally diverse subpopulations (Jennings et al., 2015), and we find that most LH GABA neurons receive inhibition from the accumbens. Large population-based recordings will be required to fully appreciate how diverse motivated behaviors are encoded by populations of NAcSh neurons. Nevertheless, moving forward, a conceptual view of the NAcSh-to-LH projection that incorporates our present observations is one that enables rapid switching between different behavioral states in response to changing external conditions.

There is a clear evolutionary requirement for neuronal circuits that can prolong or quickly stop feeding, despite immediate metabolic demands (Morton et al., 2014). However, in many societies where highly palatable and energy-dense foods are freely available, and in the absence of threat, what role can such circuits fulfill? One possibility is that maladaptive signaling within the NAcSh-to-LH pathway could contribute to feeding disorders by, for example, forcing the premature cessation of food intake in anorexia (Sunday and Halmi, 1996), or by favoring repeated and prolonged feeding bouts of palatable foods eventually causing obesity (Spiegel, 2000). More research will be necessary, but experimental evidence, taken in light of our current findings, suggests this is probable. For example, chronic restraint stress in mice that induced anorexia leading to weight loss and reduced sucrose preference was linked to altered excitatory transmission selectively onto accumbal D1R-MSNs (Lim et al., 2012). Conversely, downregulation of D1R mRNA was seen in the NAcSh of obesity-prone rats after exposure to a high-fat and high-sugar diet (Alsiö et al., 2010). How these molecular and synaptic alterations result in a functional change in the integration and firing properties of accumbal neurons that project to the LH requires further study to understand and ultimately explore rational treatment options for feeding disorders.

## EXPERIMENTAL PROCEDURES

### Animals

All experiments were reviewed by the institutional ethics committee and approved by the relevant authorities of the Canton of Geneva. Experiments

were carried out in wild-type C57BL/6J mice (bred in house or obtained from Janvier Labs) or genetically modified lines as detailed in Table S1.

### Surgery

Mice received stereotaxic injections of opsins and neural tracers and were implanted with fiber optics as described previously (Brown et al., 2012) and detailed further in the Supplemental Experimental Procedures.

### Neuronal Tracing

For CTB tracing, mice were injected with 100–200 nl CTB-488, CTB-555, or CTB-647 (AF-CTB, all from Life Technologies) unilaterally into the LH (anterior-posterior [AP]  $-1.2$ , medial-lateral [ML]  $+1.2$ , dorsal-ventral [DV]  $-4.75$ ), following surgical procedures detailed in the Supplemental Experimental Procedures. For rabies tracing, mice received stereotaxic injection of 250–400 nl AAV5-Flex-TVA-mCherry mixed with AAV8-Flex-RG unilaterally into the LH, followed by 1  $\mu$ l SAD $\Delta$ G-EFG(EnvA) into the LH 14 days later. Then, 11 days after CTB injections and 7 days after rabies injections, brains were processed for confocal imaging, as detailed in the Supplemental Experimental Procedures. To aid visualization, images were adjusted for brightness and contrast using Photoshop (Adobe), but alterations always were applied to the entire image.

### In Vitro Electrophysiology

Acute coronal 200- to 250- $\mu$ m brain slices containing NAcSh or LH were prepared in cooled artificial cerebrospinal fluid (ACSF) containing the following (in mM): NaCl 119, KCl 2.5, MgCl<sub>2</sub> 1.3, CaCl<sub>2</sub> 2.5, Na<sub>2</sub>HPO<sub>4</sub> 1.0, NaHCO<sub>3</sub> 26.2, and glucose 11, bubbled with 95% O<sub>2</sub> and 5% CO<sub>2</sub>. In older mice, slices were prepared in ACSF as above with the addition of the following (in mM): kynurenic acid 3, NaHCO<sub>3</sub>, sucrose 225, glucose 1.25, and MgCl<sub>2</sub> 4.9. Slices were kept at 34°C for 30 min before being transferred to the recording chamber superfused with 2.5 ml/min ACSF. Whole-cell patch-clamp recordings were made in NAc or LH neurons, while photocurrents were evoked by light flashes delivered from a microscope-mounted blue or orange LED (Thorlabs) through the objective, or by a blue or orange laser light directed onto the slice. The holding potentials were  $-70$  mV for NAcSh MSNs and  $-60$  mV for LH neurons, and input resistances were measured using a hyperpolarizing step of  $-4$  mV every 10 s. Traces were amplified, filtered at 5 kHz, and digitized at 10 kHz. The liquid junction potential was small and so traces were not corrected.

For validation of optogenetic effectors, the internal solution contained the following (in mM): potassium gluconate 130, MgCl<sub>2</sub> 4, Na<sub>2</sub> ATP 3.4, Na<sub>3</sub> GTP 0.1, creatine phosphate 10, HEPES 5, and EGTA 1.1. For recording light-evoked inhibitory synaptic currents in voltage-clamp mode, a high-chloride solution was used, as before but with the following (in mM): potassium gluconate 30 and KCL 100. In some experiments, GABA currents were blocked by wash in of picrotoxin (100  $\mu$ M, Tocris) and excitation was blocked by the addition of kynurenic acid (2 mM, Sigma-Aldrich). Further details on circuit mapping and biocytin labeling are provided in the Supplemental Experimental Procedures.

### Feeding Studies

All mice were first trained to consume liquid fat or sucrose over five, once daily, 1-hr sessions. Food and water were freely available in the home cage, unless otherwise stated. Food training and testing took place in four mouse operant chambers (15.9  $\times$  14  $\times$  12.7 cm; Med-Associates). Each chamber was housed in an isolated cubicle and was equipped with a contact lickometer (ENV-250, Med-Associates) that allowed for the counting of licks at a sipper tube held in one wall of the chamber. The sipper tube provided access to either sucrose (10% w/v in water) or fat (5% v/v in water of Lipofundin; from 20% Lipofundin MCT/LCT, Braun Medical). Lipofundin is a fat emulsion containing both medium and long-chain triglycerides, with an energy content of 7,990 (1,908 kJ (kcal)/l. Liquid fat was chosen for the majority of our studies, since it was consumed readily in mice without the need for food restriction and permits comparison with an extensive body of literature that has examined NAcSh and LH circuitry using either solid or liquid fat in rodents (Katsuura et al., 2011; Zhang et al., 1998; Zheng et al., 2007). Licking activity was recorded with a PC running Med-PC IV (Med-Associates) and custom code written in MEDState Notation. An individual feeding burst was defined as three or

more consecutive licks with a maximum ILI of  $\leq 1$  s. Full details of the apparatus used, including those for optogenetic manipulations, are provided in the [Supplemental Experimental Procedures](#).

### In Vivo Unit Recordings

D1RCre and D2RCre mice were injected with DIO-ChR2(H134R) in the NAcSh and implanted with a fixed-position recording electrode coupled to an optic fiber. Mice were trained to consume liquid fat and neural activity was recorded using an Omniplex system (Plexon). Signals were high-pass filtered ( $>150$  Hz). Spike sorting was performed in Offline Sorter (Plexon) with custom routines written in MATLAB used for subsequent analyses. Further details are provided in the [Supplemental Experimental Procedures](#).

To optogenetically identify D1R or D2R NAcSh neurons, 1 s of continuous blue light (0.5–2 mW at the tip of the patch cable) was delivered to the implanted fiber, as described by others (Jin et al., 2014; Kravitz et al., 2013). Cross-correlations between the average of all light-evoked and the average of all spontaneous action potential waveforms were computed. Only cells exhibiting significant light-evoked responses (Wilcoxon rank-sum test; 1 s pre versus 1 s during light), with short latencies (within 10–20 ms), and with cross-correlation values  $>0.98$  were further considered for analysis as D1R- or D2R-expressing neurons (Cohen et al., 2012).

### Statistics

Lick counts in the 1-hr daily access sessions were binned in 10-min blocks and subject to analysis by mixed-factor ANOVA, with definition of between-subject (e.g., condition, Cre+ or Cre-) and/or within-subject factors (e.g., 10-min block, 0–6; light period, on or off). Comparison of total licks was made by paired or non-paired, two-tailed Student's *t* test. For analysis of the frequency distribution of burst size during light-on and -off periods, data were first subject to a mixed-factor ANOVA analysis, with condition (e.g., Cre+ or Cre-) and light period (off or on) defined as between- and within-subject factors, respectively. Where a significant interaction between condition and light period was found ( $p \leq 0.05$ ), further between-subject comparisons were performed using a non-paired, two-tailed *t* test with Bonferroni corrections applied. Some experiments in VGaTCre and D2RCre mice were performed using a within-subject design and, as such, statistical tests were adjusted for a paired design.

To assess statistical significance of in vivo unit-recording data and to permit direct comparison with similar studies (Krause et al., 2010; Tellez et al., 2012), a Wilcoxon rank-sum test was used to compare unit activity changes during consumption onset and offset (significance level  $\leq 0.05$  and  $<0.1$  considered as a trend). Specifically, for lick onset we compared mean firing rates from the 3-s period prior to the first lick of a bout, with mean firing rates from the first 1-s period of the bout. Similarly, for lick offset we compared mean firing rates during the last 1-s period of the bout, with mean firing rates in the 3-s period following bout termination.

### SUPPLEMENTAL INFORMATION

Supplemental Information includes Supplemental Experimental Procedures, six figures, and one table and can be found with this article online at <http://dx.doi.org/10.1016/j.neuron.2015.09.038>.

### AUTHOR CONTRIBUTIONS

Behavioral experiments, neural tracing, and optogenetic-assisted circuit-mapping studies were conceived and designed by E.C.O. and C.L. E.C.O. performed and analyzed the experiments, with assistance from S.L. and M.H. for circuit mapping and V.P. for validation of optogenetic effectors. Y.K. designed, performed, and analyzed unit-recording experiments, with assistance from C.R. and E.C.O. The manuscript was written by E.C.O. and C.L. with input from all the authors.

### ACKNOWLEDGMENTS

We thank members of the C.L. laboratory and M.T.C. Brown for discussion and comments on the manuscript; S. Startchik and the Bioimaging Platform at the

University of Geneva for assistance with imaging analysis; E. Valjent for advice on immunohistochemistry; A. Holtmaat, Y. Bernardinelli, and D. Huber for providing virus constructs; and K. Deisseroth and the UNC viral vector core, Chapel Hill, for optogenetic effectors. This work was financed by a grant from the Swiss National Science Foundation, the National Center of Competence in Research (NCCR) SYNAPSY-The Synaptic Bases of Mental Diseases, and a European Research Council advanced grant (MeSSI).

Received: May 29, 2015

Revised: September 1, 2015

Accepted: September 17, 2015

Published: October 22, 2015

### REFERENCES

- Alsö, J., Olszewski, P.K., Norbäck, A.H., Gunnarsson, Z.E.A., Levine, A.S., Pickering, C., and Schiöth, H.B. (2010). Dopamine D1 receptor gene expression decreases in the nucleus accumbens upon long-term exposure to palatable food and differs depending on diet-induced obesity phenotype in rats. *Neuroscience* 171, 779–787.
- Anand, B.K., and Brobeck, J.R. (1951). Hypothalamic control of food intake in rats and cats. *Yale J. Biol. Med.* 24, 123–140.
- Aragona, B.J., Liu, Y., Yu, Y.J., Curtis, J.T., Detwiler, J.M., Insel, T.R., and Wang, Z. (2006). Nucleus accumbens dopamine differentially mediates the formation and maintenance of monogamous pair bonds. *Nat. Neurosci.* 9, 133–139.
- Baldo, B.A., and Kelley, A.E. (2007). Discrete neurochemical coding of distinguishable motivational processes: insights from nucleus accumbens control of feeding. *Psychopharmacology (Berl.)* 197, 439–459.
- Baldo, B.A., Gual-Bonilla, L., Sijapati, K., Daniel, R.A., Landry, C.F., and Kelley, A.E. (2004). Activation of a subpopulation of orexin/hypocretin-containing hypothalamic neurons by GABAA receptor-mediated inhibition of the nucleus accumbens shell, but not by exposure to a novel environment. *Eur. J. Neurosci.* 19, 376–386.
- Berthoud, H.-R. (2004). Mind versus metabolism in the control of food intake and energy balance. *Physiol. Behav.* 81, 781–793.
- Bocklisch, C., Pascoli, V., Wong, J.C.Y., House, D.R.C., Yvon, C., de Roo, M., Tan, K.R., and Lüscher, C. (2013). Cocaine disinhibits dopamine neurons by potentiation of GABA transmission in the ventral tegmental area. *Science* 341, 1521–1525.
- Brown, M.T.C., Tan, K.R., O'Connor, E.C., Nikonenko, I., Muller, D., and Lüscher, C. (2012). Ventral tegmental area GABA projections pause accumbal cholinergic interneurons to enhance associative learning. *Nature* 492, 452–456.
- Cardinal, R.N., Parkinson, J.A., Hall, J., and Everitt, B.J. (2002). Emotion and motivation: the role of the amygdala, ventral striatum, and prefrontal cortex. *Neurosci. Biobehav. Rev.* 26, 321–352.
- Cohen, J.Y., Haesler, S., Vong, L., Lowell, B.B., and Uchida, N. (2012). Neuron-type-specific signals for reward and punishment in the ventral tegmental area. *Nature* 482, 85–88.
- Cromwell, H.C., and Berridge, K.C. (1993). Where does damage lead to enhanced food aversion: the ventral pallidum/substantia innominata or lateral hypothalamus? *Brain Res.* 624, 1–10.
- de Lecea, L., Kilduff, T.S., Peyron, C., Gao, X., Foye, P.E., Danielson, P.E., Fukuhara, C., Battenberg, E.L., Gautvik, V.T., Bartlett, F.S., 2nd, et al. (1998). The hypocretins: hypothalamus-specific peptides with neuroexcitatory activity. *Proc. Natl. Acad. Sci. USA* 95, 322–327.
- Delgado, J.M.R., and Anand, B.K. (1953). Increase of food intake induced by electrical stimulation of the lateral hypothalamus. *Am. J. Physiol.* 172, 162–168.
- Faure, A., Richard, J.M., and Berridge, K.C. (2010). Desire and dread from the nucleus accumbens: cortical glutamate and subcortical GABA differentially generate motivation and hedonic impact in the rat. *PLoS ONE* 5, e11223.

- Fromentin, G., Darcel, N., Chaumontet, C., Marsset-Baglieri, A., Nadkarni, N., and Tomé, D. (2012). Peripheral and central mechanisms involved in the control of food intake by dietary amino acids and proteins. *Nutr. Res. Rev.* 25, 29–39.
- Gangarossa, G., Espallergues, J., de Kerchove d'Exaerde, A., El Mestikawy, S., Gerfen, C.R., Hervé, D., Girault, J.A., and Valjent, E. (2013). Distribution and compartmental organization of GABAergic medium-sized spiny neurons in the mouse nucleus accumbens. *Front. Neural Circuits* 7, 22.
- Heimer, L., Zahm, D.S., Churchill, L., Kalivas, P.W., and Wohltmann, C. (1991). Specificity in the projection patterns of accumbal core and shell in the rat. *Neuroscience* 41, 89–125.
- Hussain, S.S., and Bloom, S.R. (2013). The regulation of food intake by the gut-brain axis: implications for obesity. *Int. J. Obes.* 37, 625–633.
- Jennings, J.H., Rizzi, G., Stamatakis, A.M., Ung, R.L., and Stuber, G.D. (2013). The inhibitory circuit architecture of the lateral hypothalamus orchestrates feeding. *Science* 341, 1517–1521.
- Jennings, J.H., Ung, R.L., Resendez, S.L., Stamatakis, A.M., Taylor, J.G., Huang, J., Veleta, K., Kantak, P.A., Aita, M., Shilling-Scriver, K., et al. (2015). Visualizing hypothalamic network dynamics for appetitive and consummatory behaviors. *Cell* 160, 516–527.
- Jin, X., Tecuapetla, F., and Costa, R.M. (2014). Basal ganglia subcircuits distinctively encode the parsing and concatenation of action sequences. *Nat. Neurosci.* 17, 423–430.
- Katsuura, Y., Heckmann, J.A., and Taha, S.A. (2011). mu-Opioid receptor stimulation in the nucleus accumbens elevates fatty tastant intake by increasing palatability and suppressing satiety signals. *Am. J. Physiol. Regul. Integr. Comp. Physiol.* 301, R244–R254.
- Kelley, A.E., Baldo, B.A., and Pratt, W.E. (2005a). A proposed hypothalamic-striatal axis for the integration of energy balance, arousal, and food reward. *J. Comp. Neurol.* 493, 72–85.
- Kelley, A.E., Baldo, B.A., Pratt, W.E., and Will, M.J. (2005b). Corticostriatal-hypothalamic circuitry and food motivation: integration of energy, action and reward. *Physiol. Behav.* 86, 773–795.
- Kenny, P.J. (2011). Reward mechanisms in obesity: new insights and future directions. *Neuron* 69, 664–679.
- Krause, M., German, P.W., Taha, S.A., and Fields, H.L. (2010). A pause in nucleus accumbens neuron firing is required to initiate and maintain feeding. *J. Neurosci.* 30, 4746–4756.
- Kravitz, A.V., Owen, S.F., and Kreitzer, A.C. (2013). Optogenetic identification of striatal projection neuron subtypes during in vivo recordings. *Brain Res.* 1511, 21–32.
- Kupchik, Y.M., Brown, R.M., Heinsbroek, J.A., Lobo, M.K., Schwartz, D.J., and Kalivas, P.W. (2015). Coding the direct/indirect pathways by D1 and D2 receptors is not valid for accumbens projections. *Nat. Neurosci.* 18, 1230–1232.
- Lim, B.K., Huang, K.W., Grueter, B.A., Rothwell, P.E., and Malenka, R.C. (2012). Anhedonia requires MC4R-mediated synaptic adaptations in nucleus accumbens. *Nature* 487, 183–189.
- Maldonado-Irizarry, C.S., Swanson, C.J., and Kelley, A.E. (1995). Glutamate receptors in the nucleus accumbens shell control feeding behavior via the lateral hypothalamus. *J. Neurosci.* 15, 6779–6788.
- Mogenson, G.J., Swanson, L.W., and Wu, M. (1983). Neural projections from nucleus accumbens to globus pallidus, substantia innominata, and lateral preoptic-lateral hypothalamic area: an anatomical and electrophysiological investigation in the rat. *J. Neurosci.* 3, 189–202.
- Morgane, P.J. (1969). The function of the limbic and rhinic forebrain-limbic midbrain systems and reticular formation in the regulation of food and water intake. *Ann. N Y Acad. Sci.* 157, 806–848.
- Morton, G.J., Meek, T.H., and Schwartz, M.W. (2014). Neurobiology of food intake in health and disease. *Nat. Rev. Neurosci.* 15, 367–378.
- Nieh, E.H., Matthews, G.A., Allsop, S.A., Presbrey, K.N., Leppla, C.A., Wichmann, R., Neve, R., Wildes, C.P., and Tye, K.M. (2015). Decoding neural circuits that control compulsive sucrose seeking. *Cell* 160, 528–541.
- Paxinos, G., and Franklin, K.B.J. (2008). *The Mouse Brain in Stereotaxic Coordinates* (Academic Press).
- Qu, D., Ludwig, D.S., Gammeltoft, S., Piper, M., Pelleymounter, M.A., Cullen, M.J., Mathes, W.F., Przypek, R., Kanarek, R., and Maratos-Flier, E. (1996). A role for melanin-concentrating hormone in the central regulation of feeding behaviour. *Nature* 380, 243–247.
- Reynolds, S.M., and Berridge, K.C. (2001). Fear and feeding in the nucleus accumbens shell: rostrocaudal segregation of GABA-elicited defensive behavior versus eating behavior. *J. Neurosci.* 21, 3261–3270.
- Richard, J.M., and Berridge, K.C. (2011). Nucleus accumbens dopamine/glutamate interaction switches modes to generate desire versus dread: D(1) alone for appetitive eating but D(1) and D(2) together for fear. *J. Neurosci.* 31, 12866–12879.
- Roitman, M.F., Wheeler, R.A., Tiesinga, P.H.E., Roitman, J.D., and Carelli, R.M. (2010). Hedonic and nucleus accumbens neural responses to a natural reward are regulated by aversive conditioning. *Learn. Mem.* 17, 539–546.
- Sakurai, T., Amemiya, A., Ishii, M., Matsuzaki, I., Chemelli, R.M., Tanaka, H., Williams, S.C., Richardson, J.A., Kozlowski, G.P., Wilson, S., et al. (1998). Orexins and orexin receptors: a family of hypothalamic neuropeptides and G protein-coupled receptors that regulate feeding behavior. *Cell* 92, 573–585.
- Sano, H., and Yokoi, M. (2007). Striatal medium spiny neurons terminate in a distinct region in the lateral hypothalamic area and do not directly innervate orexin/hypocretin- or melanin-concentrating hormone-containing neurons. *J. Neurosci.* 27, 6948–6955.
- Schöne, C., and Burdakov, D. (2012). Glutamate and GABA as rapid effectors of hypothalamic “peptidergic” neurons. *Front. Behav. Neurosci.* 6, 81.
- Schwartz, M.W., Woods, S.C., Porte, D., Jr., Seeley, R.J., and Baskin, D.G. (2000). Central nervous system control of food intake. *Nature* 404, 661–671.
- Smith, R.J., Lobo, M.K., Spencer, S., and Kalivas, P.W. (2013). Cocaine-induced adaptations in D1 and D2 accumbens projection neurons (a dichotomy not necessarily synonymous with direct and indirect pathways). *Curr. Opin. Neurobiol.* 23, 546–552.
- Spiegel, T.A. (2000). Rate of intake, bites, and chews—the interpretation of lean-obese differences. *Neurosci. Biobehav. Rev.* 24, 229–237.
- Stratford, T.R., and Kelley, A.E. (1999). Evidence of a functional relationship between the nucleus accumbens shell and lateral hypothalamus subserving the control of feeding behavior. *J. Neurosci.* 19, 11040–11048.
- Stratford, T.R., and Wirtshafter, D. (2012). Evidence that the nucleus accumbens shell, ventral pallidum, and lateral hypothalamus are components of a lateralized feeding circuit. *Behav. Brain Res.* 226, 548–554.
- Sunday, S.R., and Halmi, K.A. (1996). Micro- and macroanalyses of patterns within a meal in anorexia and bulimia nervosa. *Appetite* 26, 21–36.
- Taverna, S., Ilijic, E., and Surmeier, D.J. (2008). Recurrent collateral connections of striatal medium spiny neurons are disrupted in models of Parkinson's disease. *J. Neurosci.* 28, 5504–5512.
- Tellez, L.A., Perez, I.O., Simon, S.A., and Gutierrez, R. (2012). Transitions between sleep and feeding states in rat ventral striatum neurons. *J. Neurophysiol.* 108, 1739–1751.
- Thompson, R.H., and Swanson, L.W. (2010). Hypothesis-driven structural connectivity analysis supports network over hierarchical model of brain architecture. *Proc. Natl. Acad. Sci. USA* 107, 15235–15239.
- Tripathi, A., Prensa, L., Cebrián, C., and Mengual, E. (2010). Axonal branching patterns of nucleus accumbens neurons in the rat. *J. Comp. Neurol.* 518, 4649–4673.
- Urstadt, K.R., Kally, P., Zaidi, S.F., and Stanley, B.G. (2013). Ipsilateral feeding-specific circuits between the nucleus accumbens shell and the lateral hypothalamus: regulation by glutamate and GABA receptor subtypes. *Neuropharmacology* 67, 176–182.
- van Kerkhof, L.W.M., Trezza, V., Mulder, T., Gao, P., Voorn, P., and Vanderschuren, L.J.M.J. (2014). Cellular activation in limbic brain systems during social play behaviour in rats. *Brain Struct. Funct.* 219, 1181–1211.

- van Zessen, R., Phillips, J.L., Budygin, E.A., and Stuber, G.D. (2012). Activation of VTA GABA neurons disrupts reward consumption. *Neuron* 73, 1184–1194.
- Watabe-Uchida, M., Zhu, L., Ogawa, S.K., Vamanrao, A., and Uchida, N. (2012). Whole-brain mapping of direct inputs to midbrain dopamine neurons. *Neuron* 74, 858–873.
- Wickersham, I.R., Finke, S., Conzelmann, K.-K., and Callaway, E.M. (2007). Retrograde neuronal tracing with a deletion-mutant rabies virus. *Nat. Methods* 4, 47–49.
- Wise, R.A. (1974). Lateral hypothalamic electrical stimulation: does it make animals 'hungry'? *Brain Res.* 67, 187–209.
- Zhang, M., Gosnell, B.A., and Kelley, A.E. (1998). Intake of high-fat food is selectively enhanced by mu opioid receptor stimulation within the nucleus accumbens. *J. Pharmacol. Exp. Ther.* 285, 908–914.
- Zhang, J.-P., Xu, Q., Yuan, X.-S., Cherasse, Y., Schiffmann, S.N., de Kerchove d'Exaerde, A., Qu, W.-M., Urade, Y., Lazarus, M., Huang, Z.-L., and Li, R.X. (2013). Projections of nucleus accumbens adenosine A2A receptor neurons in the mouse brain and their implications in mediating sleep-wake regulation. *Front. Neuroanat.* 7, 43.
- Zheng, H., Corkern, M., Stoyanova, I., Patterson, L.M., Tian, R., and Berthoud, H.-R. (2003). Peptides that regulate food intake: appetite-inducing accumbens manipulation activates hypothalamic orexin neurons and inhibits POMC neurons. *Am. J. Physiol. Regul. Integr. Comp. Physiol.* 284, R1436–R1444.
- Zheng, H., Patterson, L.M., and Berthoud, H.-R. (2007). Orexin signaling in the ventral tegmental area is required for high-fat appetite induced by opioid stimulation of the nucleus accumbens. *J. Neurosci.* 27, 11075–11082.
- Zheng, H., Lenard, N.R., Shin, A.C., and Berthoud, H.-R. (2009). Appetite control and energy balance regulation in the modern world: reward-driven brain overrides repletion signals. *Int. J. Obes.* 33 (Suppl 2), S8–S13.